All polarization-maintaining Er fiber-based optical frequency combs with nonlinear amplifying loop mirror

N. Kuse,[1,*] J. Jiang,[1] C.-C. Lee,[2] T. R. Schibli,[2] and M.E. Fermann[1]

[1] IMRA America Inc., 1044 Woodridge Avenue, Ann Arbor, MI, 48105, USA
[2] Department of Physics, University of Colorado at Boulder, 2000 Colorado Avenue, Boulder, Colorado 80309-0390, USA
[*]nkuse@imra.com

Abstract: A fully stabilized all polarization-maintaining Er frequency comb with a nonlinear amplifying loop mirror with below 0.2 rad carrier-envelope-offset frequency phase noise is demonstrated. The integrated timing jitter is measured as 40 attosecond from 10 kHz to 10 MHz, which is the lowest value of any Er fiber frequency comb to date.

©2016 Optical Society of America

OCIS codes: (140.4050) Mode-locked lasers; (140.3425) Laser stabilization; (140.3500) Lasers, erbium.

References and links

1. S. A. Diddams, D. J. Jones, J. Ye, S. T. Cundiff, J. L. Hall, J. K. Ranka, R. S. Windeler, R. Holzwarth, T. Udem, and T. W. Hänsch, "Direct link between microwave and optical frequencies with a 300 THz femtosecond laser comb," Phys. Rev. Lett. **84**(22), 5102–5105 (2000).
2. S. A. Diddams, "The evolving optical frequency comb," J. Opt. Soc. Am. B **27**(11), B51–B62 (2010).
3. N. R. Newbury, "Searching for applications with a fine-tooth comb," Nat. Photonics **5**(4), 186–188 (2011).
4. B. R. Washburn, S. A. Diddams, N. R. Newbury, J. W. Nicholson, M. F. Yan, and C. G. Jørgensen, "Phase-locked, erbium-fiber-laser-based frequency comb in the near infrared," Opt. Lett. **29**(3), 250–252 (2004).
5. T. R. Schibli, I. Hartl, D. C. Yost, M. J. Martin, A. Marcinkevicius, M. E. Fermann, and J. Ye, "Optical frequency comb with submillihertz linewidth and more than 10 W average power," Nat. Photonics **2**(6), 355–359 (2008).
6. C. C. Lee, C. Mohr, J. Bethge, S. Suzuki, M. E. Fermann, I. Hartl, and T. R. Schibli, "Frequency comb stabilization with bandwidth beyond the limit of gain lifetime by an intracavity graphene electro-optic modulator," Opt. Lett. **37**(15), 3084–3086 (2012).
7. M. Hofer, M. E. Fermann, F. Haberl, M. H. Ober, and A. J. Schmidt, "Mode locking with cross-phase and self-phase modulation," Opt. Lett. **16**(7), 502–504 (1991).
8. I. Hartl, L. Dong, M. E. Fermann, T. R. Schibli, A. Onae, F.-L. Hong, H. Inaba, K. Minoshima, and H. Matsumoto, "Long-term carrier envelope phase locking of a PM fiber frequency comb source," Optical Fiber Communication Conference (OSA, 2005), paper OFJ2.
9. E. Baumann, F. R. Giorgetta, J. W. Nicholson, W. C. Swann, I. Coddington, and N. R. Newbury, "High-performance, vibration-immune, fiber-laser frequency comb," Opt. Lett. **34**(5), 638–640 (2009).
10. L. C. Sinclair, I. Coddington, W. C. Swann, G. B. Rieker, A. Hati, K. Iwakuni, and N. R. Newbury, "Operation of an optically coherent frequency comb outside the metrology lab," Opt. Express **22**(6), 6996–7006 (2014).
11. N. Kuse, C.-C. Lee, J. Jiang, C. Mohr, T. R. Schibli, and M. E. Fermann, "Ultra-low noise all polarization-maintaining Er fiber-based optical frequency combs facilitated with a graphene modulator," Opt. Express **23**(19), 24342–24350 (2015).
12. M. E. Fermann, F. Haberl, M. Hofer, and H. Hochreiter, "Nonlinear amplifying loop mirror," Opt. Lett. **15**(13), 752–754 (1990).
13. I. N. Duling, "All-fiber ring soliton laser mode locked with a nonlinear mirror," Opt. Lett. **16**(8), 539–541 (1991).
14. N. J. Doran and D. Wood, "Nonlinear-optical loop mirror," Opt. Lett. **13**(1), 56–58 (1988).
15. C.-C. Lee, S. Suzuki, W. Xie, and T. R. Schibli, "Broadband graphene electro-optic modulators with sub-wavelength thickness," Opt. Express **20**(5), 5264–5269 (2012).
16. D. D. Hudson, K. W. Holman, R. J. Jones, S. T. Cundiff, J. Ye, and D. J. Jones, "Mode-locked fiber laser frequency-controlled with an intracavity electro-optic modulator," Opt. Lett. **30**(21), 2948–2950 (2005).
17. Y. Nakajima, H. Inaba, K. Hosaka, K. Minoshima, A. Onae, M. Yasuda, T. Kohno, S. Kawato, T. Kobayashi, T. Katsuyama, and F. L. Hong, "A multi-branch, fiber-based frequency comb with millihertz-level relative linewidths using an intra-cavity electro-optic modulator," Opt. Express **18**(2), 1667–1676 (2010).
18. J. W. Nicholson and M. Andrejco, "A polarization maintaining, dispersion managed, femtosecond figure-eight fiber laser," Opt. Express **14**(18), 8160–8167 (2006).

19. G. D. Cole, W. Zhang, M. J. Martin, J. Ye, and M. Aspelmeyer, "Tenfold reduction of Brownian noise in high-reflectivity optical coatings," Nat. Photonics **7**(8), 644–650 (2013).
20. B. J. Bloom, T. L. Nicholson, J. R. Williams, S. L. Campbell, M. Bishof, X. Zhang, W. Zhang, S. L. Bromley, and J. Ye, "An optical lattice clock with accuracy and stability at the 10^{-18} level," Nature **506**(7486), 71–75 (2014).
21. I. Ushijima, M. Takamoto, M. Das, T. Ohkubo, and H. Katori, "Cryogenic optical lattice clocks," Nat. Photonics **9**(3), 185–189 (2015).
22. T. M. Fortier, M. S. Kirchner, F. Quinlan, J. Taylor, J. C. Bergquist, T. Rosenband, N. Lemke, A. Ludlow, Y. Jiang, C. W. Oates, and S. A. Diddams, "Generation of ultrastable microwave via optical frequency division," Nat. Photonics **5**(7), 425–429 (2011).
23. K. Jung, J. Shin, and J. Kim, "Ultralow phase noise microwave generation from mode-locked Er-fiber lasers with subfemtosecond integrated timing jitter," IEEE Photonics J. **5**(3), 5500906 (2013).
24. C. Aguergaray, R. Hawker, A. F. J. Runge, M. Erkintalo, and N. G. R. Broderick, "120 fs, 4.2 nJ pulses from an all-normal-dispersion, polarization-maintaining, fiber laser," Appl. Phys. Lett. **103**(12), 121111 (2013).
25. J. Szczepanek, T. M. Kardaś, M. Michalska, C. Radzewicz, and Y. Stepanenko, "Simple all-PM-fiber laser mode-locked with a nonlinear loop mirror," Opt. Lett. **40**(15), 3500–3503 (2015).
26. G. C. Valley, "Photonic analog-to-digital converters," Opt. Express **15**(5), 1955–1982 (2007).
27. H. Kim, P. Qin, Y. Song, H. Yang, J. Shin, C. Kim, K. Jung, C. Wang, and J. Kim, "Sub-20-attosecond timing jitter mode-locked fiber lasers," IEEE J. Quantum Electron. **20**(5), 0901108 (2013).
28. T. K. Kim, Y. Song, K. Jung, C. Kim, H. Kim, C. H. Nam, and J. Kim, "Sub-100-as timing jitter optical pulse trains from mode-locked Er-fiber lasers," Opt. Lett. **36**(22), 4443–4445 (2011).
29. C. Kim, S. Bae, K. Kieu, and J. Kim, "Sub-femtosecond timing jitter, all-fiber, CNT-mode-locked Er-laser at telecom wavelength," Opt. Express **21**(22), 26533–26541 (2013).
30. T. R. Schibli, J. Kim, O. Kuzucu, J. T. Gopinath, S. N. Tandon, G. S. Petrich, L. A. Kolodziejski, J. G. Fujimoto, E. P. Ippen, and F. X. Kaertner, "Attosecond active synchronization of passively mode-locked lasers by balanced cross correlation," Opt. Lett. **28**(11), 947–949 (2003).
31. J. Kim, J. Chen, Z. Zhang, F. N. C. Wong, F. X. Kärtner, F. Loehl, and H. Schlarb, "Long-term femtosecond timing link stabilization using a single-crystal balanced cross correlator," Opt. Lett. **32**(9), 1044–1046 (2007).
32. H. Lin, D. K. Donald, and W. V. Sorin, "Optimizing polarization states in a figure-8 laser using a nonreciprocal phase shifter," J. Lightwave Technol. **12**(7), 1121–1128 (1994).
33. M. E. Fermann, M. Hofer, F. Haberl, A. J. Schmidt, and L. Turi, "Additive-pulse-compression mode locking of a neodymium fiber laser," Opt. Lett. **16**(4), 244–246 (1991).
34. S. Namiki and H. A. Haus, "Noise of the stretched pulse fiber laser: part I—theory," IEEE J. Quantum Electron. **33**(5), 649–659 (1997).
35. R. Paschotta, "Timing jitter and phase noise of mode-locked fiber lasers," Opt. Express **18**(5), 5041–5054 (2010).

1. Introduction

As optical frequency combs become increasingly established in a plethora of applications in many different areas [1–3], it is becoming increasingly clear that robust comb systems are imperative to solidify the advancements of recent years. Among the various comb architectures investigated to date, fiber-based frequency combs still stand out because of the unique combination of compact size, well established manufacturability and high performance they can offer [4–6]. Most fiber-based frequency combs rely on nonlinear polarization rotation (NPR) [7] to achieve a high level of performance. Frequency combs based on NPR rarely need alignment once they are aligned properly. However, frequency combs based on NPR are sensitive to changes in environmental condition such as temperature, pressure and vibration, which lead to polarization changes, a reduction in comb performance and can result in even a complete loss of mode-locking. This means that although frequency combs based on NPR can be used inside laboratories, they are not suitable for applications in the field. To overcome this difficulty, all polarization maintaining (PM) fiber-based frequency combs have been studied [8–11]. To realize all PM fiber-based frequency combs, one has essentially the choice of two methods: saturable absorber (SA) based mode-locking [10, 11] or the exploitation of Kerr based amplitude modulation mechanisms such as possible with a nonlinear amplifying loop mirror (NALM) [12, 13] (or nonlinear optical loop mirror (NOLM [14])). Very recently, we reported an all PM low noise Er frequency comb with a semiconductor saturable absorber mirror (SESAM), which incorporated a graphene modulator (GM) [6, 15] and electro-optic modulator (EOM) [16, 17] to stabilize f_{ceo} and f_{beat} with large feedback bandwidths [11]. However, the optical spectrum was limited by the relaxation time of the SESAM, resulting in larger intrinsic phase noise of f_{ceo} and timing jitter than achievable with frequency combs based on NPR. A frequency comb with a NALM is a promising candidate to realize both an all PM configuration and intrinsic

low noise. Although all PM frequency combs with a NALM (also called "figure 8") are reported [9, 18], the initiation of mode-locking was challenging; i.e. mode-locking needed to be started with an intra-cavity electro-optic modulator. In addition, the demonstrated phase noise of the phase locked f_{ceo} was more than 1 rad, which may not be sufficient for optical clocks comprising a sub-Hz linewidth reference laser [19–21] or for applications of the comb for low noise RF generation [22, 23]. Without additional cavity modulation, a coupler with a large asymmetric ratio can be employed for self-starting mode-locking [24, 25]. However, such asymmetry causes additional loss, which is not suitable for operation with low intrinsic noise.

Not only phase noise of phase locked f_{ceo} and f_{beat}, but also free-running timing jitter is important, because well designed fiber lasers can operate with sufficiently low free-running timing jitter to be applied to microwave generation [22, 23] and high-speed photonic analog-to-digital converters [26] without the need for any phase locking. Sub 100 as timing jitter was demonstrated with fiber lasers using NPR, specifically sub 20 as for Yb fiber lasers [27] and 70 as for Er fiber lasers [28]. However, timing jitter of lasers based on NPR is very sensitive to even slight changes of environmental conditions, and as a result such lasers need daily adjustments of waveplates. Mode-locked laser with SAs are more reliable, but have much worse timing jitter [29]. Thus, an all PM frequency comb, which is very robust and at the same time offers low timing jitter is highly sought.

In this work, we demonstrate a self-starting all PM fiber-based frequency combs with a NALM optimized with the incorporation of an additional phase bias. As in [11], we use a GM and an EOM to stabilize f_{ceo} and f_{beat} simultaneously with large feedback bandwidths, and obtain an integrated phase noise of 0.16 rad and 0.13 rad for f_{ceo} and f_{beat}, respectively. In addition, we measured the timing jitter of an all PM fiber-based frequency combs for the first time by using the balanced optical cross-correlation (BOC) method, which enables to measure attosecond timing jitter and has been applied to high resolution timing jitter measurement [30, 31]. The measured integrated timing jitter is about 40 as integrated from 10 kHz to 10 MHz, which is the lowest value for any Er fiber frequency comb to date. This demonstrates that all PM fiber-based frequency combs based on a NALM can have lower intrinsic noise compared to frequency combs based on NPR. We believe the present all PM frequency comb combines a robust system architecture with ultra low noise performance and will be very attractive for even the most demanding comb applications.

2. Function of phase bias

An appropriate phase bias, which consists of the combination of two Faraday rotators and a waveplate [32], assists the mode-locking induced by the NALM. We discuss two cavity designs. One consists of two loops; NALM and circular loop (also referred to as Fig. 8 laser), as shown in Fig. 1(a). The other consists of NALM and linear arm, as shown in Fig. 1(b) [33]. Without any phase bias and nonlinear phase offset between clockwise (cw) and counter-clockwise (ccw), the optical loop reflects the light, i.e. the light from an input port is reflected back to the input port. Therefore, in the case of Fig. 1(a), cavity loss for CW laser states becomes largest because of an isolator and, in the case of Fig. 1(b), cavity loss for CW laser states becomes smallest without any phase bias and nonlinear phase difference as shown dashed lines in Figs. 1(a) and 1(b). In the case of Fig. 1(a), a π nonlinear phase offset between cw and ccw propagation in the NALM is required to obtain mode-locking without any phase bias. Because of this, additional cavity modulation such as active mode-locking is often necessary to initiate passive mode-locking. By applying a phase bias in the NALM, the required nonlinear phase offset can be mitigated. For example, if a $\delta\phi$ phase bias is applied, the required nonlinear phase offset becomes $\delta\phi$ or $\pi - \delta\phi$. Thus, initiating mode-locking with a phase bias is easier than without phase bias. Figure 1(b) is a schematic of our laser reported in this paper. The advantage of this setup compared with Fig. 1(a) is that a reflective modulator such as the GM or a mirror with PZT can be easily installed, and a higher repetition frequency is possible. However, mode-locking without any phase bias will not occur for this configuration, because without any nonlinear phase offset, the CW laser state

always has less cavity loss than a mode-locking state. The phase bias can shift the minimum point of cavity loss, which makes the cavity loss of the mode-locking state smaller than that of the CW laser state. For example, if a $\delta\phi$ phase bias is applied, the nonlinear phase offset of $\delta\phi$ or $\pi - \delta\phi$ can initiate mode-locking.
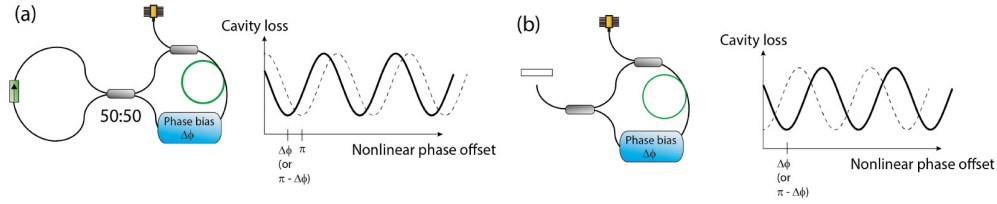

Fig. 1. (a) (left) Schematic of an oscillator with two loops and (right) cavity loss dependent on nonlinear phase offset. Black line and dotted black line show the cavity loss with and without the phase bias. (b) (left) Schematic of an oscillator with NALM and linear arm and (right) cavity loss dependent on nonlinear phase offset. Black line and dotted black line show the cavity loss with and without the phase bias.

3. Oscillator

Figure 2 shows the schematic of the oscillator, which consists of a linear arm based on free-space, which can be integrated by using a micro-optic package, and a NALM part. All compenents are PM, including couplers, Er doped fiber, and non doped fiber. In the linear arm part, a GM and bulk EOM are installed for fast control of f_{ceo} and f_{beat} (or f_{rep}), respectively. Note that although a GM is used as a satuable absorber for some mode-locked lasers, our GM is designed for f_{ceo} control [6, 15] and actually mode-locking can be obtained without the GM. In the NALM, a phase bias, PZT and EDFA are installed. The PZT is attached to a fiber for slow control of f_{beat} (or f_{rep}). The EDFA is put on a copper plate on a Peltier device, which is used for very slow control of f_{beat} (or f_{rep}). The oscillator has two output ports. The output power from each port is a few mW, which infers the same intracavity power as all PM Er fiber frequency combs with SESAM [11], when pumped with about 150 mW at 976 nm. The repetition frequency is about 83 MHz. The dispersion is set slightly negative by using positive dispersion Er doped-fiber and negative dispersion non doped fiber. Output spectra from each port are shown in Fig. 2(b). The FWHM is about 30 nm and 40 nm for output 1 and output 2, respectively, corresponding to Fourier transform-limited pulse duration of a 110 fs and 100 fs, respectively. The obtained spectral width is twice larger than achieved with all PM Er frequency combs with a SESAM [11]. Thus, we can expect lower intrinsic phase noise of f_{ceo} and timing jitter, because the quantum-limited timing jitter power spectrum density (PSD) is proportional to the pulse duration squared [34].
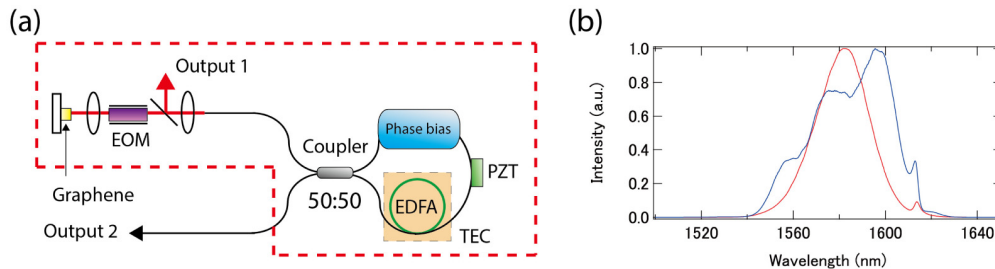

Fig. 2. (a) Schematic of the oscillator. EOM, electro-optic modulator; PZT, piezo transducer; EDFA, erbium-doped fiber amplifier; TEC, temperature controller. (b) Optical spectra from output 1 (red) and output 2 (blue).

4. Phase locking of f_{ceo} and f_{beat}

To observe the f_{ceo}, a PM Er amplifier and a PM highly nonlinear fiber (HNLF) are installed after the oscillator [Fig. 3(a)]. More details are shown in [11]. As shown in Fig. 3(b), more than 45 dB signal-to-noise ratio (SNR) at 100 kHz resolution bandwidth (RBW) is obtained. f_{beat} is obtained by interfering optically bandpass filtered output 2 and a single longitudinal mode CW laser specified with about a wavelength of 1559 nm and a linewidth of 2 kHz.

For f_{ceo} phase locking, the GM and pump current modulation are used. Although the GM has large feedback bandwidth, the modulation range is too small to keep phase locking for the long term. Thus, pump current modulation is also employed. For f_{beat} phase locking, the EOM, PZT, and fiber TEC are used. A fiber TEC is required, since the tuning range of f_{beat} by the PZT is not enough to keep phase locking for extended time periods.

Figures 3(c) and 3(e) show the in-loop RF spectrum and PSD of phase locked f_{ceo} and f_{beat} by using PI^{2}D loop filters. For f_{ceo}, the feedback bandwidth is more than 1 MHz according to the servo bump, which would be limited by the phase delay of the feedback loop, caused by GM response, optical and electric path lengths, and electric components. For f_{beat}, the feedback bandwidth is about 500 kHz, which is limited by the EOM response. A bulk EOM is used, but a waveguide EOM [9] can improve the feedback bandwidth, although a waveguide EOM has larger loss. Because of the large feedback bandwidth, more than 50 dB coherent peaks at 3 kHz RBW are obtained for both f_{ceo} and f_{beat}. The PSDs and integrated phase noise of f_{ceo} and f_{beat} are shown in Figs. 3(d) and 3(f). 0.16 rad of integrated phase noise of f_{ceo} from 1 Hz to 3 MHz is obtained, which is lower than in recently demonstrated all PM Er frequency combs [11]. This is because the intrinsic phase noise of an all PM Er frequency comb with a NALM is smaller than that of an all PM Er frequency comb with a SESAM.

For future practical applications, we also demonstrated long term phase locking. Because pump current modulation for f_{ceo} and TEC for f_{beat} provide a much larger modulation depth than long term fluctuation of those signals under our laboratory conditions (which are subject to around $\pm$ 2 degree C temperature fluctuations), phase locking can be preserved essentially indefinitely. The results are shown in Figs. 3(g) and 3(h). Long term locking without any phase slips was kept for a few days. Standard deviations for f_{ceo} and f_{beat} are estimated to be about 460 µHz, and 240 µHz, respectively. Note that phase locking was intentionally stoped to pursue other experiments.
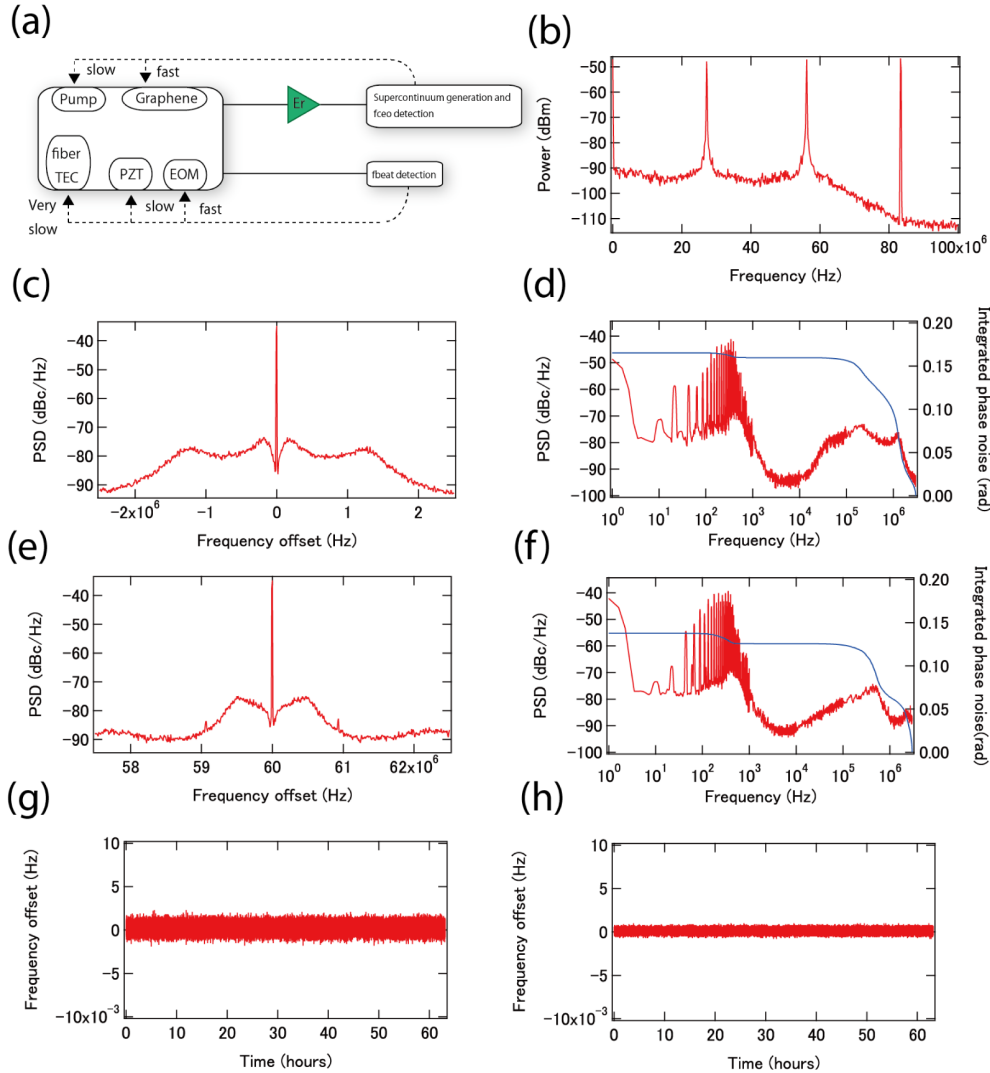
Fig. 3. (a) The schematic of comb setup. (b) In-loop RF spectrum of free-running f_{ceo} with 100 kHz RBW. (c) In-loop RF spectrum of phase locked f_{ceo} with 3 kHz RBW. (d) In-loop PSD and integrated phase noise of phase locked f_{ceo}. (e) In-loop RF spectrum of phase locked f_{beat} with 3 kHz RBW. (f) In-loop PSD and integrated phase noise of phase locked f_{beat}. (g) Frequency of phase locked f_{ceo}. (h) Frequency of phase locked f_{beat}.

5. Timing jitter

To evaluate the utility of the present system as a precision timing reference, the timing jitter was measured using a BOC. For timing jitter measurement, two almost identical lasers are prepared. One has a GM and bulk EOM. The other has only a PZT attached to the end mirror in the linear arm. Note that f_{rep} for this experiment is about 72 MHz instead of 83 MHz for experimental convenience, and the dispersion is more carefully adjusted to become closer to zero. The measurement setup is similar to [31], as shown in Fig. 4(a). A 4 mm length of type II PPKTP is used to generate the sum frequency generation (SFG) between two lasers. The linear slope of the BOC signal is used as an error signal to lock two separate, but near identical lasers at zero time delay. The feedback bandwidth of the PZT was set to about 6 kHz, allowing us to measure the free-running timing jitter above 6 kHz. To calibrate the error

signal measured in voltage PSD (V²/Hz) to jitter PSD (fs²/Hz), the two lasers are locked with a 10 Hz repetition frequency difference. Then, multiple BOC signals are observed separated by 100 ms, which can be used as a time reference. By averaging the time separation between multiple BOC signals, a more accurate conversion coefficient of mV/fs can be obtained. The measured double-sided jitter PSD is shown in Fig. 4(b). From 20 kHz to 400 kHz, the jitter PSD is proportional to $1/f^2$. Above 3 MHz, the jitter PSD is limited by photodetector noise. The integrated timing jitter is estimated to be about 40 as integrated from 10 kHz to 10 MHz. Here, the same and uncorrelated timing jitter of those two lasers is assumed, and a division factor of 2 is implemented. The black line in Fig. 4(b) shows the theoretical quantum-limited timing jitter, estimated by using equation below [35].

$$L(f) = 0.53 \frac{\theta h \nu}{P_{avg}} \left(f_{rep} \tau_p \right)^2 l_{total} \frac{1}{(2\pi f)^2} \qquad (1)$$

Here, $L(f)$ is the double-sided timing jitter PSD, θ is the excess noise factor, $h\nu$ is the photon energy, P_{avg} is intracavity average power, τ_p is the FWHM pulse duration, l_{total} is the cavity loss per round trip, and f is the frequency offset. The coefficient of 0.53 assumes $sech^2$ pulse shapes. To calculate the theoretical jitter, the measured intracavity average power of 50 mW, a pulse duration of 100 fs, an excess noise factor of 3, and total intracavity losses per round trip of 50% were used. The measured jitter is slightly larger than the theoretical quantum-limited timing jitter because of other timing jitter sources such as Gordon-Haus timing jitter. The obtained jitter is the lowest for any Er frequency comb demonstrated to date.
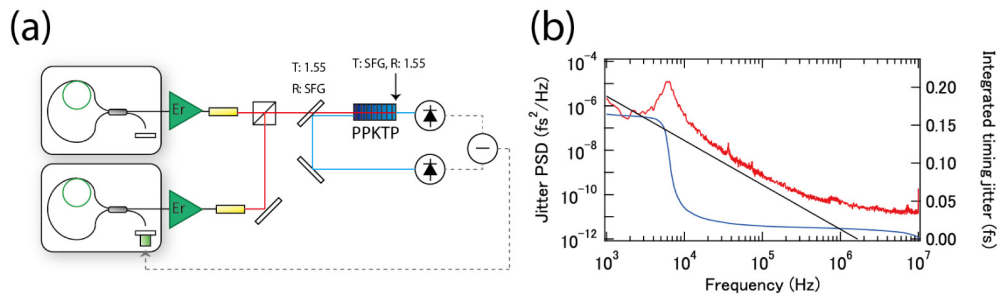

Fig. 4. (a) The schematic of measurement setup for BOC. (b) Jitter PSD for the laser (red) and theoretical estimation (black) and integrated timing jitter (blue).

6. Conclusion

In conclusion, we demonstrated all PM Er frequency comb incorporating a NALM with the phase bias. The obtained phase noise of phase locked f_{ceo} (0.16 rad) was better than with a recently demonstrated low noise all PM Er frequency comb with a SESAM (0.25 rad) because of lower intrinsic phase noise, benefitting from the use of a fast artificial saturable absorber, i.e. a NALM. In addition, timing jitter was measured for the first time for an all PM fiber laser. The obtained timing jitter is the lowest of any Er fiber laser demonstrated to date, including fiber lasers based on NPR. We believe that ultra low phase noise frequncy combs as demonstrated here, which are principally more robust and reproducible than non PM fiber lasers, will greatly expand the application potential of frequency comb technology.

Note added in proof: with a further optimized system we recently achieved 35/30 mrad for f_{ceo}/f_{beat} in-loop phase noise integrated from 100 Hz to 2 MHz. After submission of the manuscript, W. Hänsel et. al, reported another all PM low phase noise Er fiber optical frequency comb at a conference (W. Hänsel et.al., ATh4A, ASSL 2015), although no details of the Er oscillator were not shown.

Acknowledgments